



# Preparation of chitosan microcarriers by high voltage electrostatic field and freeze drying

Zekang Lu, Yan Zhou, and Baolin Liu\*

*Institute of Biothermal Engineering, University of Shanghai for Science and Technology, Shanghai 200093, China*

Received 18 October 2018; accepted 31 March 2019

Available online 24 April 2019

**In this paper, a biocompatible, non-toxic porous chitosan microcarrier was prepared by high voltage electrostatic field and freeze drying technology. The chitosan solution was pushed from the syringe drop into the sodium polyphosphate solution using a booster pump. The droplet diameter of the chitosan solution was adjusted by the voltage of the electrostatic field formed between the syringe and the sodium polyphosphate solution. The droplets were dropped into a sodium polyphosphate solution to form microspheres. The microspheres were subsequently immersed in 25% (v/v) glutaraldehyde for crosslinking to enhance the mechanical strength of the microspheres. These microspheres were then frozen and lyophilized to form a microcarrier. By performance characterization, these microcarriers had a particle size of 400–500  $\mu\text{m}$ , a pore size of 15–20  $\mu\text{m}$ , and a porosity of 90%. Under simulated human environmental conditions, the 21-day degradation rate was about 30%, indicating that the microcarriers have potential clinical value.**

© 2019, The Society for Biotechnology, Japan. All rights reserved.

[**Key words:** Chitosan; Porous; Microcarriers; High-voltage electrostatic field; Freeze drying]

Bio-hybrid artificial livers made from isolated hepatocytes and polymer microcarriers are of great significance for the treatment of liver failure. However, one of the key issues to use it in tissue engineering or cell therapy is to obtain a sufficient number of cells by amplifying small biopsy samples. Monolayer cell culture provides a convenient and efficient method for amplifying the number of cells, but during cell culture, most of the cell phenotype is lost, and the biochemical characteristics of the extracellular matrix are altered (1). A few studies (2,3) tested two-dimensional models under static conditions, but did not mimic the physiological conditions of cells *in vivo*. Therefore, microcarriers with biocompatibility, biodegradability, uniform interconnection and highly open porous structure are expected to be ideal scaffold carriers. The microcarriers not only achieve sufficient cell seeding density on the surface and inside, but also allow nutrient and oxygen to enter and exit, which contributes to subsequent cell proliferation and differentiation. Furthermore, cell microcarriers can be cultured in suspension.

Hepatocytes have been cultured in artificial liver using a variety of synthetic microcarriers, including the poly lactic-co-glycolic acid (PLGA) family (4,5). They not only provide a large surface area for cell attachment, but also make suspension culture possible. However, these microcarriers are not biocompatible and therefore are not suitable for clinical use. Chitosan is a partially deacetylated derivative of chitin, which is biodegradable, biocompatible and non-toxic (6). It is a linear polysaccharide consisting of  $\beta 1 \rightarrow 4$  linked D-glucosamine residues with a variable number of randomly located N-acetyl-glucosamines. Studies have

shown that porous chitosan scaffolds enhance several liver-specific functions in hepatocytes cultured *in vitro*, such as albumin secretion and urea synthesis (7–9).

Several methods have previously been developed to prepare three-dimensional porous microcarriers, including emulsions, suspensions, homogenization and freeze drying (10,11). Emulsion polymerization is one of the most commonly used methods. However, it does not control the diameter and homogenization of the microcarriers. In addition, some special solvents or compounds such as hexafluoroisopropanol, hexafluoroacetone or chlorohydrin need to be added to the emulsion. Thus, it would result in potential toxicity. In order to solve these problems, a new method for preparing chitosan microcarriers is proposed in this study, which employs high voltage electrostatic field technology and freeze drying. The chitosan microcarrier prepared by this method has uniform shape, good mechanical stability, excellent hydrophilicity and biodegradability, and has potential clinical application value.

## MATERIALS AND METHODS

**Strategy of experimentation** Both artificial liver and liver transplantation require a large amount of hepatocyte source. Compared with traditional single-layer plates, microcarriers have good mass transfer ability and mechanical stability, and can provide a larger specific surface area for hepatocyte culture. In addition, the microcarriers provides a three-dimensional growth space for the cells, which are more conducive to protecting the normal function of the cells and facilitating high-quality, high-density culture of the hepatocytes. Currently common microcarrier materials are not biocompatible, therefore not suitable for clinical use. Moreover, the preparation methods of the common porous microcarriers often fail to control the size of the microcarriers, and some methods require addition of some chemical substances, resulting in

\* Corresponding author. Tel./fax: +86 21 55270702.

E-mail address: [blliuk@163.com](mailto:blliuk@163.com) (B. Liu).

potential toxicity. This paper aims to prepare a three-dimensional porous microcarrier which can precisely control the size and morphology of microcarriers by using chitosan as the raw material by combining high-voltage electrostatic technology with freeze-drying technology.

**Experimental design** Chitosan microcarriers were prepared by high-voltage electrostatic technology, and the microcarriers were made into a porous structure by freeze-drying technique, and the size, surface structure and internal structure of the porous microcarriers were measured. Next, the water absorption and porosity of the porous microcarriers were measured and calculated respectively. Finally, hepatocyte culture experiments and in vitro degradation experiments of microcarriers were carried out.

**Preparation of chitosan microspheres** Microspheres were prepared by a high-voltage pulse microcarriers molding instrument (University of Shanghai for Science and Technology, Shanghai, China). The schematic of the device is shown in Fig. 1.

Two grams, two and a half grams and three grams of chitosan were weighed and dissolved in 100 ml of 1% acetic acid solution to prepare chitosan solution with concentration of 2% (w/v), 2.5% (w/v), and 3% (w/v). Then, the chitosan solution was placed in a water bath thermostat (Shanghai Hualian Medical Instrument Co., Ltd., Shanghai, China) at 37°C for 24 h, and then kept at room temperature without any treatment until the bubbles disappeared. Sodium polyphosphate solutions of pH 4, 7, and 10 were prepared by dissolving different amounts of sodium polyphosphate (MW 367.86, Sinopharm Chemical Reagent Co., Ltd., Shanghai, China) in distilled water. A blunt end needle with a diameter of 0.7 mm was used. As shown in Fig. 1, the negative lead of the high voltage generator (Huatae Electric Co., Ltd., Wuhan, China) was connected to the syringe needle and the positive lead was connected to the copper ring placed at the bottom of the beaker. The high voltage generator and the syringe pump were turned on to form a high voltage pulse electric field between the needle and the bead copper ring. Under the dual action of the electric field force and the driving force of the syringe pump, the chitosan acid solution overcomes the viscous force and surface tension, and drops into the sodium polyphosphate solution in the beaker at a certain particle size. The chitosan acid solution reacts with the sodium polyphosphate solution and solidifies to form chitosan/sodium polyphosphate microspheres.

These microspheres were washed in distilled water and immersed in 25% (v/v) glutaraldehyde for 90 min to stabilize. The obtained microcarriers were washed three times with distilled water, and the microcarriers were collected by centrifugation at 4000 rpm for 10 min at 4°C. The microcarriers were stored in a 4°C refrigerator until used in further experiments.

**Preparation of porous chitosan microcarriers** Through the above operation, the most suitable microspheres are selected for lyophilization to prepare porous chitosan microcarriers.

Different cooling rates and final temperatures will result in microcarriers with different properties. After the experiment, the pre-cooling temperature and the cooling rates were determined. The microcarriers were frozen in a programmable freezer (University of Shanghai for Science and Technology) to -20°C or -40°C and then held for 2 h. The remaining microcarriers were placed in a low temperature refrigerator (Sanyo, Osaka, Japan) at -80°C. And set the cooling rate constant at 1°C/min.

We transfer the pre-frozen chitosan microcarriers to a pre-cooled lyophilizer and set the shelf temperature for initial drying. Based on the measured eutectic temperature of the chitosan microcarriers, the shelf temperature was set at -20°C and the vacuum was controlled at 10–30 Pa. After several tests, the average value of the initial drying time was calculated to be 10 h.

Based on multiple tests, the shelf temperature during the secondary drying process was set at 10°C. The water vapor pressure in the system decreases as the moisture of the microcarriers escapes, which weakens the heat transfer process. In

order to shorten the secondary drying time and bring the carrier to the highest allowable temperature as quickly as possible, the pressure of secondary drying was increased to 15–30 Pa. When the temperature of the microcarrier reaches 10°C, the degree of vacuum is restored, allowing residual moisture to escape. After the test, the secondary drying time was determined to be about 2 h.

In summary, the frozen microcarriers were rapidly transferred to a pre-cooled freeze dryer (Virtis Corporation, Warminster, PA, USA) for lyophilization. About 90%–95% of the microcarrier solvent was removed during the preliminary drying (10 h at -20°C), and almost all of the solvent was removed during the second drying (2 h at 10°C). Fig. 2 shows the freeze-drying curve.

**Size, surface morphology and internal structures of microcarriers** In order to observe the size, surface morphology and internal structure of the microcarriers by scanning electron microscopy (S50, FEI, Hillsboro, OR, USA), the dried microcarriers were frozen in liquid nitrogen and cut into slices with a surgical knife. These slices were mounted on a metal stub and coated with gold at a thickness of 20 nm using a sputter coater (12). The size distribution, diameter and pore size were averaged from five different microcarriers.

**The water uptake ratio (γ) of microcarriers** The dried microcarriers were washed in 70% ethanol, then washed three times with cold deionized water, and finally incubated in phosphate buffer for 12 h. The excess water was removed from the surface using absorbent paper. The water uptake ratio was calculated by the following equation:

$$\gamma(\%) = (W_w - W_d) / W_d \times 100\% \tag{1}$$

where  $W_w$  and  $W_d$  are the wet weight and dry weight of the microcarriers, respectively.

**The porosity (ε) of microcarriers** The porosity of the chitosan microcarriers was measured by liquid displacement method (13). Pure ethanol was used as the replacement liquid because it does not cause the matrix to expand or contract when penetrating into the microcarrier. The microcarriers (dry weight,  $W_w$ ) were immersed in a known volume ( $V_1$ ) of pure ethanol in a graduated cylinder for 5 min. The total volume of pure ethanol and pure ethanol impregnated microcarriers was recorded as  $V_2$ . The pure ethanol-impregnated microcarriers were then removed from the cylinder and the residual pure ethanol volume was recorded as  $V_3$ . The total volume of the microcarriers impregnated with pure ethanol was

$$V = (V_2 - V_1) + (V_2 - V_3) = V_2 - V_3 \tag{2}$$

where  $V_2 - V_1$  is the volume of the microcarriers and  $V_1 - V_3$  is the volume of pure ethanol within the microcarriers. The porosity ( $\epsilon$ ) of the microcarrier was obtained by

$$\epsilon(\%) = (V_1 - V_3) / (V_2 - V_3) \times 100\% \tag{3}$$

**In vitro biodegradability (ζ)** The microcarriers were incubated at 37°C in 6 well culture plates containing 1.5 μg ml<sup>-1</sup> lysozyme in phosphate buffered saline (PBS) (pH 7.4). The microcarriers were taken out from the culture medium after 7, 14, and 21 days, washed with distilled water, and lyophilized. The degradability ratio ζ was calculated as follows:

$$\zeta = (W_o - W_t) / W_o \times 100\% \tag{4}$$

where  $W_o$  denotes the original weight and  $W_t$  is the weight at day  $t$ .

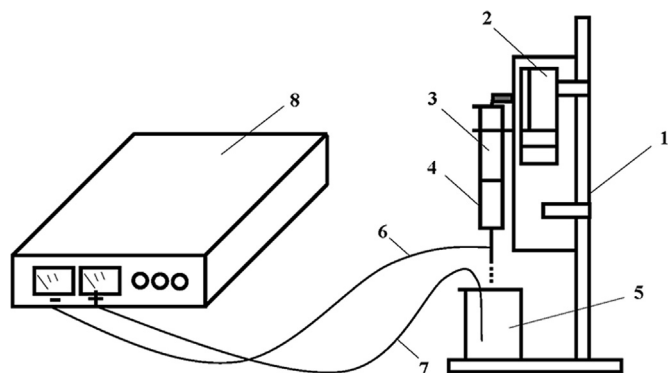


FIG. 1. The schematic representation of high-voltage pulse microcarriers molding instrument. 1, iron stand; 2, injection pump; 3, chitosan solution; 4, injector; 5, sodium polyphosphate solution; 6, negative line; 7, positive line; 8, high voltage generator.

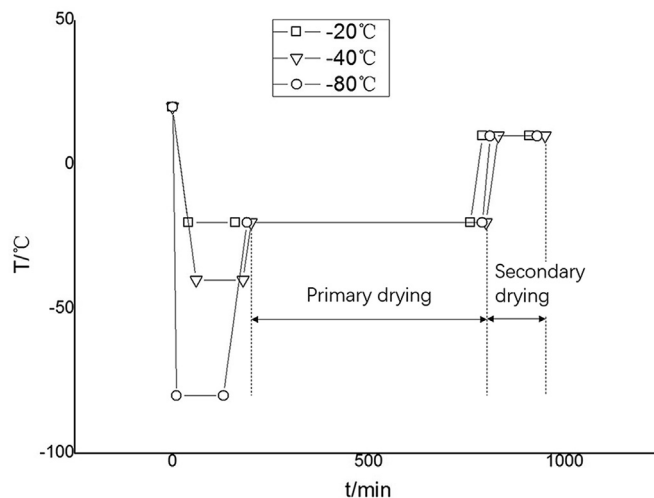


FIG. 2. The freeze-drying curve.

**TABLE 1.** Effect of chitosan concentration and pH of sodium polyphosphate on microcarriers characteristics.

Concentration of chitosan solution [% (w/v)]	pH of sodium polyphosphate	Characters of microcarriers	Size ( $\mu\text{m}$ )
2	4	Hollow microcarriers, regular surface, bad rigidity	400–800
2	7	Solid microcarriers, regular surface, bad rigidity,	400–800
2	10	Solid microcarriers, regular surface, bad rigidity	400–800
2.5	4	Hollow microcarriers, regular surface, bad rigidity,	400–500
2.5	7	Solid microcarriers, regular surface, bad rigidity	400–500
2.5	10	Solid microcarriers, regular surface, good rigidity, homogeneous	400–500
3	4	Hollow microcarriers, irregular surface, bad rigidity, inhomogeneous	$\geq 800$ or $\leq 100$
3	7	Solid microcarriers, irregular surface, bad rigidity, inhomogeneous	$\geq 800$ or $\leq 100$
3	10	Solid microcarriers, irregular surface, good rigidity, inhomogeneous	$\geq 800$ or $\leq 100$

**Culture of hepatocytes** We inoculated human hepatocytes L-02 (Shanghai Institute of Biochemistry and Cell Biology, CAS) on microcarriers for culture. The main processes of inoculation include silicification of the culture dish, microcarrier sterilization, and small volume inoculation of hepatocytes.

**Morphology observation of hepatocytes** The morphology of hepatocytes was observed dynamically using an inverted light microscope (Nikon, Osaka, Japan) and a laser confocal microscope (Nikon). The cell solution was added to a 24-well

plate and 100  $\mu\text{l}$  of 10 mg/ml acridine orange was added to each well. The 24-well plates were then placed under the laser confocal microscope. The excitation light source had a wavelength of 488 nm and the received light wavelength was 530–550 nm.

**Albumin secretion function assay of hepatocytes** The supernatants of the hepatocyte culture solutions of days 1, 2, 3, 4 and 5 and the supernatant of the control group were collected. Each sample was placed in a sample tube containing

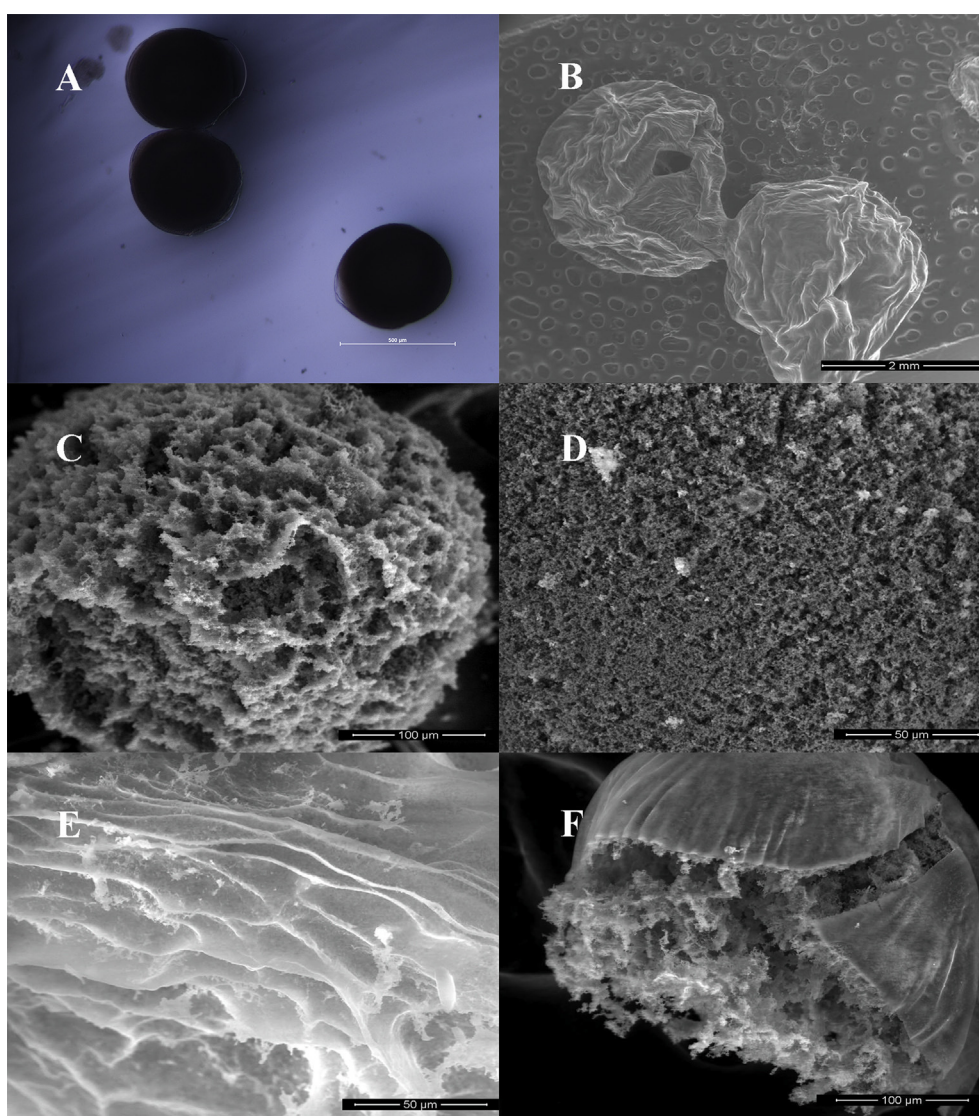


**FIG. 3.** Images of chitosan microcarriers. (A) Chitosan solution with a concentration of 2.5% (w/v) crosslinking with  $\text{Na}_5\text{P}_3\text{O}_{10}$  (pH = 10). Scale bar: 500  $\mu\text{m}$ . (B) Chitosan solution with a concentration of 3% (w/v) crosslinking with  $\text{Na}_5\text{P}_3\text{O}_{10}$  (pH = 7). Scale bar: 2 mm. (C, D) Chitosan solution with a concentration of 2.5% (w/v) crosslinking with  $\text{Na}_5\text{P}_3\text{O}_{10}$  (pH = 10) and lyophilized at  $-40^\circ\text{C}$ . Scale bars: 100  $\mu\text{m}$  (C) and 50  $\mu\text{m}$  (D). (E) Chitosan solution with a concentration of 2.5% (w/v) crosslinking with  $\text{Na}_5\text{P}_3\text{O}_{10}$  (pH = 10) and lyophilized at  $-20^\circ\text{C}$ . Scale bar: 50  $\mu\text{m}$ . (F) Chitosan solution with a concentration of 2.5% (w/v) crosslinking with  $\text{Na}_5\text{P}_3\text{O}_{10}$  (pH = 7) and lyophilized at  $-40^\circ\text{C}$ . Scale bar: 100  $\mu\text{m}$ .

physiological saline and standard albumin (4 g/dl) at a ratio of 1:1:1. One and a half milliliter of the succinic acid buffer solution (pH = 4.2) containing bromocresol green (0.15 mmol/L) and polyoxyethylene lauryl ether (30%) was added to the sample tube, and after mixing, the reaction was carried out at 25°C for 5 min. Two hundred microliters of the above solution was added to a 96-well microtiter plate. The absorbance of the sample and the standard reagent at the wavelength of 630 nm is  $A_{\text{sample}}$  and  $A_{\text{standard}}$ , respectively. The formula for calculating the albumin concentration ( $C$ ) in the sample is as follows:

$$C = \left( \frac{A_{\text{sample}}}{A_{\text{standard}}} \right) \times C_{\text{standard}} \quad (5)$$

where  $C$  is the albumin concentration (g/dl),  $C_{\text{standard}}$  is the standard albumin concentration (g/dl),  $A_{\text{sample}}$  and  $A_{\text{standard}}$  are the absorbance of the sample and the standard reagent.

**Statistical analysis** The data was processed by the statistical software SPSS, and the chart was produced using Origin V8.0. Data were expressed as mean  $\pm$  standard deviation, and  $t$ -test was used for comparison between groups.  $P < 0.05$  was considered statistically significant.

## RESULTS

**Preparation of chitosan microcarriers** Through experience summarization and single factor experiments, the factors affecting the preparation of microspheres are voltage, frequency, propulsion speed, pulse, liquid-surface distance and solution concentration. According to the experimental results, a voltage of 55 kV, a frequency of 90 Hz, a propulsion speed of 90 mm/h, a pulse width of 6 ms, and a liquid surface distance of 25 mm were selected for the preparation of microcarriers. Orthogonal experiments were carried out on the solution concentration.

The effects of chitosan concentration and pH of sodium polyphosphate on microcarriers properties are shown in Table 1. The solid microcarriers with regular surface and good rigidity were obtained when the concentration of chitosan solution was 2.5% (w/v) and the pH of the sodium polyphosphates was adjusted to 10. The size of this type solid microcarriers was between 400 and 500  $\mu\text{m}$  (Fig. 3A). However, if the pH of the sodium polyphosphate was less than 7, the microcarriers remained hollow with poor rigidity, thus easy to break (Fig. 3B). When the concentration of the chitosan solution was 3% (w/v), the microcarriers were not easily ejected from the needle. When the pH of the sodium polyphosphate was adjusted to 10 and the freezing temperature was  $-40^\circ\text{C}$ , the chitosan microcarriers had a pore size of 15–20  $\mu\text{m}$  and were evenly distributed on the surface (Fig. 3C and D). When the freezing temperature was  $-20^\circ\text{C}$ , the pore size became too large and uneven, and looked like a strip as shown in Fig. 3E. When the freezing temperature was  $-80^\circ\text{C}$ , the microcarriers were severely collapsed. However, as shown in Fig. 3F, when the pH of the sodium polyphosphate was less than 7, the microcarriers had only internal pores and the surface was smooth and free of pores. Therefore, we believe that when the concentration of chitosan solution is 2.5% (w/v) and the pH of sodium polyphosphate solution is 10, the prepared microspheres can meet the requirements of this experiment.

**Water uptake ratio and porosity of chitosan microcarriers** The hydrophilicity of microcarriers is one of the key features for evaluating artificial liver biomaterials. Thus, hydrophilicity is important for humoral absorption and cellular metabolite transfer.

As shown in Fig. 4, the water absorption of the chitosan microcarriers increased with increasing chitosan concentration and time, indicating that the chitosan microcarriers have excellent hydrophilicity. By calculating the porosity of the chitosan microcarrier by Eq. 3, it can be inferred that the porosity increases as the water absorption increases. It can be seen that the porosity of the chitosan microcarrier increases as the pre-cooling temperature decreases, and increases as the concentration of the chitosan solution

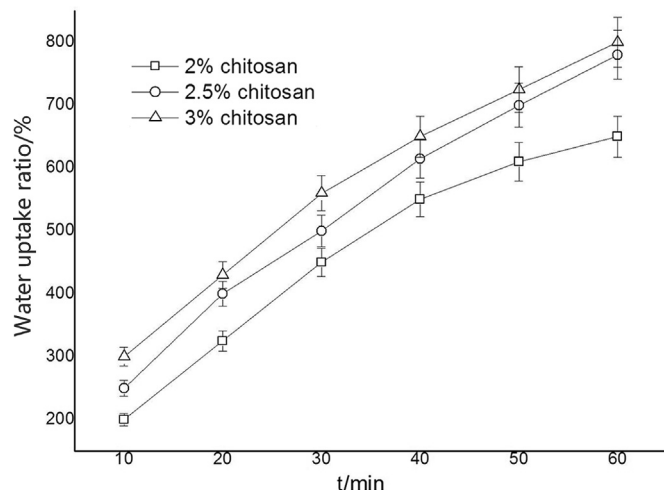


FIG. 4. Water uptake ratio of different concentrations of chitosan microcarriers.

increases. The optimal porosity of chitosan microcarriers was close to 90%. Therefore, based on SEM images and data analysis, it can be concluded that the optimal preparation method of chitosan microcarriers is to crosslink sodium polyphosphate (pH = 10) with 2.5% (w/v) chitosan and freeze at  $-40^\circ\text{C}$ .

**Biodegradability** The biodegradability of the chitosan microcarriers prepared by the above optimal protocol in lysozyme PBS solution is shown in Fig. 5. It can be seen that the chitosan microcarriers have an almost 30% weight loss on day 21.

**Morphology observation of hepatocytes** Fig. 6A shows that hepatocyte L-02 adheres and spreads on the surface of the chitosan microcarrier. When the surface of the microcarrier is overgrown with cells, part of the microcarriers were observed to be in clusters. The combination of fluorescein acridine orange with intracellular DNA and RNA allows the DNA to be bright green and the RNA to be orange-red. As can be seen from Fig. 6B, the cells on the surface of the microcarriers showed a bright green and orange-red plaque distribution, indicating that L-02 cells grew well on the surface of the microcarriers and that DNA and RNA synthesis was active.

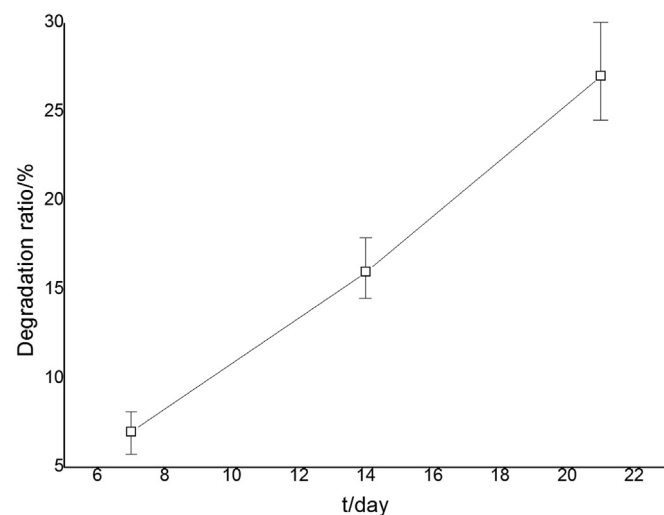


FIG. 5. Degradation of chitosan microcarriers in lysozyme PBS solution.

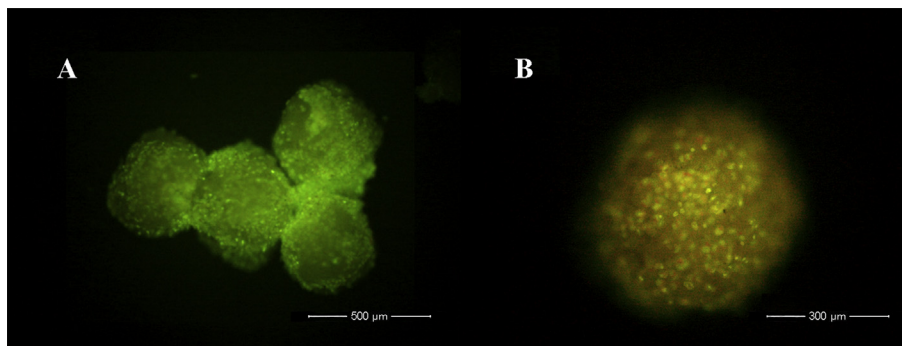


FIG. 6. Fluorescent microscope images of microcarriers. (A) Growth morphology of cells on the microcarriers. Scale bar: 500  $\mu\text{m}$ . (B) Fluorescent labeling of hepatocytes on the microcarriers. Scale bar: 300  $\mu\text{m}$ .

**Albumin secretion function assay of hepatocytes** Fig. 7 shows that albumin content continued to rise on days 1, 2 and 3, and reached the highest on day 4 and gradually decreased on day 5, which may be related to maximum cell proliferation density. There was no significant difference in albumin concentration values between the experimental groups ( $P > 0.05$ ). Therefore, we believe that chitosan microcarriers have good cytocompatibility with hepatocyte L-02, and hepatocytes L-02 can grow well on the surface of microcarriers with good cell function.

## DISCUSSION

Liver is a highly organized structure. Once the primary hepatocytes are removed from an organism, tissue-specific functions are rapidly lost. Artificial liver is important for the treatment of fulminant hepatic failure. High-density culture of hepatocytes is vital for the development of artificial liver. The emergence of various microcarriers has made it possible to culture large numbers of hepatocytes. Piskin et al. (14) prepared poly-hydroxymethylsiloxanes (PDMS-OH) microcarriers by suspension polymerization, and the prepared microcarriers with a diameter of about 200  $\mu\text{m}$ . Gabler et al. (15) used emulsification method to prepare PLGA microcarriers. The size of the resulting microcarriers was between 40 and 330  $\mu\text{m}$  by controlling the polymer concentration and stirring speed.

Surprisingly, none of the available methods precisely control the size of microcarriers, which hampers the practical applications. In order to mimic *in vivo* microenvironment for hepatocytes cultured

*in vitro*, various manufacturing techniques have been developed to produce highly porous (>90%) microcarriers for use in artificial livers. Shastri et al. (16) utilized solid hydrocarbon compounds as porogens. Kim et al. (17) prepared ammonium PLGA microspheres by double emulsion technique using ammonium bicarbonate as a porogen. Saska et al. (18) used a combination of 3D printing and selective laser sintering (SLS) to prepare poly-3-hydroxybutyrate microcarriers with a pore size of 500–700  $\mu\text{m}$ . In addition, there are methods such as freeze drying, solvent evaporation, salt impregnation, and gas foaming (13,19–22). Micromachining techniques have also been commonly used to construct two- or three-dimensional stents (23–25). However, most of these methods are still limited by their need for random microgeometry or synthetic polymers, which makes it difficult to prepare microcarriers with good tissue properties from natural materials. In this paper, chitosan porous microcarriers with a size between 400 and 500  $\mu\text{m}$  and a pore size between 15 and 20  $\mu\text{m}$  were prepared by a combination of high-voltage electrostatic technology and freeze-drying technique. By adjusting various parameters of the high pressure pulsed microcarrier molding apparatus, the fabrication of the microcarriers was precisely controlled in a high pressure field. Therefore, the diameter, uniformity and surface morphology of the microcarriers could be controlled within the desired range. The concentration of the chitosan solution and the pH of the sodium polyphosphate are two important factors affecting the appearance, rigidity and size of the microcarrier. By adjusting these two important factors, the microcarriers had a good shape. The ice crystals formed during the preparation of the microcarriers were removed by controlling various parameters in the freeze drying technique, such as freezing temperature, primary drying temperature, and secondary drying temperature. In addition, the pore structure and porosity of the porous microcarrier can be controlled by changing the above parameters. Moreover, this method does not require additional organic materials to reduce toxicity.

Our single factor experiment showed that when the voltage was lower than 50 kV, the particle size of the microspheres slowly decreased with increasing voltage. In contrast, after the voltage was higher than 50 kV, the particle size of the microspheres rapidly decreased with increasing voltage. However, if the voltage was too high, despite the smaller particle size, the particle size distribution of the microspheres was not uniform. These results point to the possibility that a voltage range between 50 and 60 kV is optimal for preparation of the microcarriers.

The pulse width affects the particle size and uniformity of the microspheres. As the pulse width is greater than 10 ms, the particle size of the microspheres is significantly increased, but the uniformity of the microspheres is poor. The pulse width is controlled in the range of 5–10 ms, and the average particle diameter of the microspheres is small and the distribution is relatively uniform.

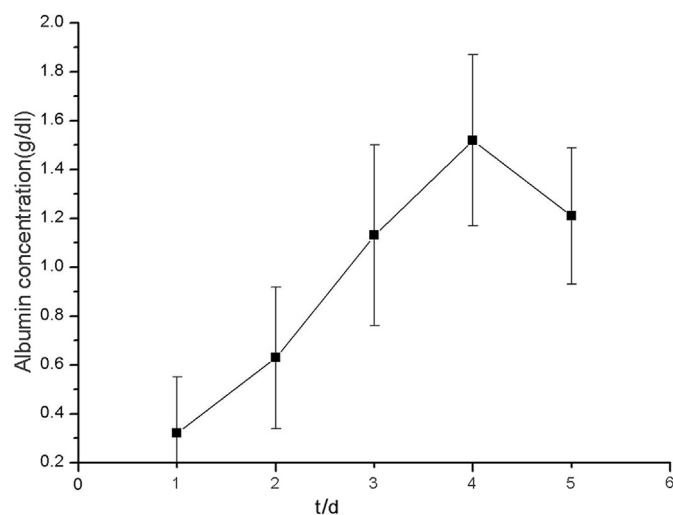


FIG. 7. Albumin secretion from hepatocytes.

After the pulse width is less than 5 ms, although the particle size can be optimally selected and the uniformity is good, microsphere adhesion occurs.

The particle size of the microspheres also decreased as the propulsion speed decreased. A small propulsion speed ensures good uniformity of the microcarriers. As the propulsion speed increases, the average particle size of the microspheres is still within a reasonable range, but significant tailing and sticking occur. In addition, the size of the frequency also affects the uniformity of the microspheres. The higher the frequency, the better the uniformity of the microspheres. Therefore, the experimental conditions were determined to be: a voltage of 55 kV, a pulse width of 6 ms, a propulsion speed of 90 mm/h, a frequency of 90 Hz, and a liquid surface distance of 25 mm.

In lyophilization process, in addition to the initial drying and secondary drying, the pre-freezing section is also important. The pre-freezing temperature will affect whether the material forms a glass state, affecting the lyophilization rate and lyophilization quality of the material. Therefore, the pre-freezing temperature should be lower than the glass transition temperature. In addition, the rate of the pre-freezing determines the appearance and structure of the material after lyophilization. The slower pre-freezing rate results in a larger crystal lattice that contributes to an increase in lyophilization efficiency. As the pre-freezing rate is increased, a smaller crystal lattice is formed, which causes cross-resistance during ice crystal sublimation, which is not conducive to lyophilization. Then the pre-freezing temperature was set at  $-40^{\circ}\text{C}$  and performed pre-freezing experiments at a rate of  $0.1^{\circ}\text{C}/\text{min}$ ,  $1^{\circ}\text{C}/\text{min}$  and  $10^{\circ}\text{C}/\text{min}$ . After the experiment, the pre-freezing speed was selected at  $1^{\circ}\text{C}/\text{min}$ .

In conclusion, we have developed a simple method for preparing three-dimensional porous microcarriers by combining high-voltage electrostatic field technology with a freeze-drying method. The microcarrier prepared by the method has a particle diameter of 400–500  $\mu\text{m}$ , a pore diameter of 15–20  $\mu\text{m}$ , a porosity of 90% and a water absorption rate of more than 300%. Under simulated human environmental conditions, the 21-day degradation rate was approximately 30%. The chitosan microcarrier prepared by the novel method has excellent performance and can be used as a potential scaffold for further development of artificial liver.

#### ACKNOWLEDGMENTS

This work was supported by the National Natural Science Foundation of China, No. 51776130.

#### References

- Von der Mark, K., Gauss, V., Von der Mark, H., and Muller, P.: Relationship between cell shape and type of collagen synthesised as chondrocytes lose their cartilage phenotype in culture. *Nature*, **267**, 531–532 (1977).
- Kaeffer, B. and Briollais, S.: Primary culture of colonocytes in rotating bioreactor. *In Vitro Cell. Dev. Biol. Anim.*, **34**, 622–625 (1998).
- Barralet, J. E., Wang, L., Lawson, M., Triffitt, J. T., Cooper, P. R., and Shelton, R. M.: Comparison of bone marrow cell growth on 2D and 3D alginate hydrogels. *J. Mater. Sci. Mater. Med.*, **16**, 515–519 (2005).
- Nam, Y. S., Yoon, J. J., and Park, T. G.: A novel fabrication method of macroporous biodegradable polymer scaffolds using gas foaming salt as a porogen additive. *J. Biomed. Mater. Res.*, **53**, 1–7 (2000).
- Cusick, R. A., Lee, H., Sano, K., Pollok, J. M., Utsunomiya, H., Ma, P. X., Langer, R., and Vacanti, J. P.: The effect of donor and recipient age on engraftment of tissue-engineered liver. *J. Pediatr. Surg.*, **32**, 357–360 (1997).
- Suh, J. K. and Matthew, H. W.: Application of chitosan-based polysaccharide biomaterials in cartilage tissue engineering: a review. *Biomaterials*, **21**, 2589–2598 (2000).
- Li, J., Pan, J., Zhang, L., Guo, X., and Yu, Y.: Culture of primary rat hepatocytes within porous chitosan scaffolds. *J. Biomed. Mater. Res. A*, **67**, 938–943 (2003).
- Elcin, Y. M., Dixit, V., and Gitnick, G.: Hepatocyte attachment on biodegradable modified chitosan membranes: in vitro evaluation for the development of liver organoids. *Artif. Organs*, **22**, 837–846 (1998).
- Young, B. R., Pitt, W. G., and Cooper, S. L.: Protein adsorption on polymeric biomaterials I. Adsorption isotherms. *J. Colloid Interface Sci.*, **124**, 28–44 (1998).
- Lim, S. T., Martin, G. P., Berry, D. J., and Brown, M. B.: Preparation and evaluation of the in vitro drug release properties and mucoadhesion of novel microspheres of hyaluronic acid and chitosan. *J. Control. Release*, **66**, 281–292 (2000).
- Yuyama, H., Yamamoto, K., Shirafuji, K., Nagai, M., Ma, G. H., and Omi, S.: Preparation of polyurethaneurea (PUU) uniform spheres by SPG emulsification technique. *J. Appl. Polym. Sci.*, **77**, 2237–2245 (2000).
- Li, K., Wang, Y., Miao, Z., Xu, D., Tang, Y., and Feng, M.: Chitosan/gelatin composite microcarrier for hepatocyte culture. *Biotechnol. Lett.*, **26**, 879 (2004).
- Kim, U.-J., Park, J., Kim, H. J., Wada, M., and Kaplan, D. L.: Three-dimensional aqueous-derived biomaterial scaffolds from silk fibroin. *Biomaterials*, **26**, 2775–2785 (2005).
- Piskin, E., Denkbaz, E. B., and Hoffman, A. S.: Silicone-based microcarriers: preparation and BHK cell culture. *Chem. Eng. J. Biochem. Eng. J.*, **58**, 65–70 (1995).
- Gabler, F., Frauenschuh, S., Ringe, J., Brochhausen, C., Götz, P., Kirkpatrick, C. J., Sittinger, M., Schubert, H., and Zehbe, R.: Emulsion-based synthesis of PLGA-microspheres for the in vitro expansion of porcine chondrocytes. *Biomol. Eng.*, **24**, 515–520 (2007).
- Shastri, V. P., Martin, I., and Langer, R.: Macroporous polymer foams by hydrocarbon templating. *Proc. Natl. Acad. Sci. USA*, **97**, 1970–1975 (2000).
- Kim, T. K., Yoon, J. J., Lee, D. S., and Park, T. G.: Gas foamed open porous biodegradable polymeric microspheres. *Biomaterials*, **27**, 152–159 (2006).
- Saska, S., Pires, L. C., Cominotte, M. A., Mendes, L. S., Oliveira, M. F., Maia, I. A., Silva, J. V. L., Riberiro, S. J. L., and Cirelli, J. A.: Three-dimensional printing and in vitro evaluation of poly(3-hydroxybutyrate) scaffolds functionalized with osteogenic growth peptide for tissue engineering. *Mater. Sci. Eng. C*, **89**, 265–273 (2018).
- Mooney, D. J., Kaufmann, P. M., Sano, K., Mcnamara, K. M., Vacanti, J. P., and Langer, R.: Transplantation of hepatocytes using porous biodegradable sponges. *Transplant. Proc.*, **26**, 3425–3426 (1994).
- Lv, Q., Feng, Q., Hu, K., and Cui, F.: Three-dimensional fibroin/collagen scaffolds derived from aqueous solution and the use for HepG2 culture. *Polymer*, **46**, 12662–12669 (2005).
- Khanna, H. J., Klein, M. D., and Matthew, H. W. T.: Novel design of a chitosan-collagen scaffold for hepatocyte implantation, pp. 1295–1298, in: International Conference of the IEEE Engineering in Medicine & Biology Society, vol. 2. IEEE (2000).
- Swornakumari, C., Meignanalakshmi, S., Legadevi, R., and Palanisammi, A.: Preparation of microspheres using poly-3-hydroxybutyrate biopolymer and its characterization. *J. Environ. Biol.*, **39**, 331–338 (2018).
- Leclerc, E., Furukawa, K. S., Miyata, F., Sakai, Y., Ushida, T., and Fujii, T.: Fabrication of microstructures in photosensitive biodegradable polymers for tissue engineering applications. *Biomaterials*, **25**, 4683–4690 (2004).
- Bettinger, C. J., Weinberg, E. J., Kulig, K. M., Vacanti, J. P., Yadong, W., Borenstein, J. T., and Langer, R.: Three dimensional microfluidic tissue-engineering scaffolds using a flexible biodegradable polymer. *Adv. Mater.*, **18**, 65–69 (2006).
- Kaixuan, Z., Yunru, Y., Yue, C., Conghui, Tian, Gang, Z., and Yuanjin, Zhao: All-Aqueous-phase microfluidics for cell encapsulation. *ACS Appl. Mater. Interfaces*, **11**, 4826–4832 (2019).